

# Limit analysis of brick masonry shear walls with openings under later loads by rigid block modeling

**F. Portioli, L. Cascini, R. Landolfo**

*University of Naples "Federico II", Italy*

**P. Foraboschi**

*IUAV University, Venice, Italy*



## SUMMARY:

This paper describes an application of rigid block limit analysis to masonry shear walls with openings supported by experimental investigation. A simplified micro-modelling approach was used to develop the model, based on the idealization of masonry units and joints with rigid blocks separated by contact interfaces. To characterize the behaviour at interfaces, crushing and sliding failure were considered. For sliding, different flow rules were used, including associative and non-associative friction laws. The limit analysis problem was formulated and solved by means of linear programming. To solve the limit analysis problem a computer program was developed. To evaluate the accuracy of the used modelling procedure, the rigid block model of the perforated shear walls was validated against experimental tests and a sensitivity analysis was carried out to assess the influence of various parameters and modelling assumptions on the predicted response.

*Keywords: Brick masonry wall, opening, limit analysis, iterative linear programming.*

## 1. INTRODUCTION

The application of mathematical programming to the rigid block limit analysis of masonry structures has received a growing attention from researchers in the last decades. Various are the reasons of this increasing interest in the authors' opinion. Among them, the straightforward formulation of the limit analysis problem in terms of mathematical programming, the development of new solution methods to non-linear problems as well as the availability of robust algorithms for the solution of large scale problems, such as interior point methods.

In rigid block limit analysis, the structure is discretized into a number of rigid blocks interacting through joints. Failure, which generally involves separation, sliding and crushing, can occur at block interfaces. The problem is formulated at the block and joint level in terms of equilibrium and kinematic equations as well as in terms of yield functions and flow rules, that is considering the internal forces and displacement rates at interfaces.

Both micro and macro-modelling strategies are possible depending on the complexity and size of the investigated masonry structure. In the first case, each stone unit is modelled with a block while the behaviour of mortar and mortar-unit interfaces is lumped into a single joint. In macro-modelling approach, whole masonry parts are modelled with blocks interacting at joints which represent potential cracks in the structure (Orduna 2003).

In this paper, a simplified micro-modelling approach with rigid blocks is used to investigate the behaviour of mortared brick masonry shear walls with opening under later loads. The walls under investigation were tested at the IUAV to assess the effects of interlocking and sliding on the behaviour of the panels (Foraboschi 2009).

The main aim of the study is to assess the capability of rigid block limit analysis in predicting the experimental response and to assess the sensitivity of the results to different modelling parameters and assumptions, including material model characteristics, friction flow rule and macro-modelling approaches.

In the next sections the details of the implemented modelling procedure are presented. The results of

the numerical analysis on the perforated walls are presented and compared with experimental tests to show the accuracy of the modelling approach and implemented solution procedure. Parametric analysis were carried out to assess the sensitivity of the model to material properties and level of vertical load. Modelling strategies and simplifications, such as the use of simplified micro-modelling or the use of a single block for the lintel are discussed as well.

Comparison of associate and non-associate solutions are presented and discussed on the basis of experimental results.

## 2. THE RIGID BLOCK LIMIT ANALYSIS MODEL

In this section, the main details of the modelling approach used to formulate the limit analysis problem as a mathematical program are provided. Static and kinematic variables as well as equilibrium equations, constitutive laws and flow rules are presented in matrix form.

The formulation of governing equations, which mainly refers to the works by Ferris & Tin Loi (2001) and Orduña & Lourenço (2005), was developed for two-dimensional block assemblages and is based on equilibrium formulation of rigid blocks which involves the maximization of upper bound solutions to the limit analysis problem.

### 2.1. Static and kinematic variables

The static variables are represented by the internal forces acting at the interface  $j$  and referred to the centre of the joint, that are  $V_j$ ,  $N_j$ ,  $M_j$  (Fig. 1). These variables are organized in the vector  $\mathbf{x}_j$ .

$$\mathbf{x}_j = \begin{bmatrix} V_j \\ N_j \\ M_j \end{bmatrix}. \quad (2.1)$$

The corresponding kinematic variables are the relative displacement rates at the interfaces (Fig. 2). These variables are collected in the vector  $\mathbf{q}_j$ :

$$\mathbf{q}_j = \begin{bmatrix} \gamma_j \\ \varepsilon_j \\ \omega_j \end{bmatrix}. \quad (2.2)$$

The loads are applied to the centroid of the rigid block  $i$  and are indicated with the vector  $\mathbf{f}_i$ :

$$\mathbf{f}_i = \begin{bmatrix} f_{xi} \\ f_{yi} \\ m_i \end{bmatrix}. \quad (2.3)$$

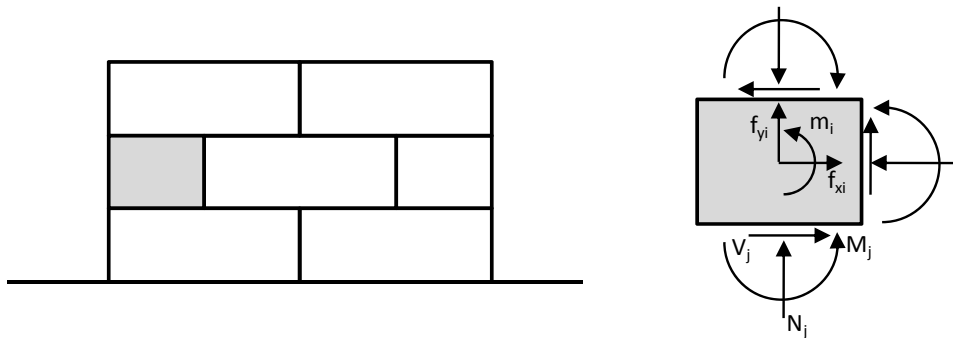


Figure 1. Joint and block static variables

The loads  $\mathbf{f}_i$  can be expressed as the sum of the known dead loads  $\mathbf{f}_{Di}$  and live loads  $\mathbf{f}_{Li}$  amplified by an unknown scalar multiplier  $\alpha$ .

$$\mathbf{f}_i = \mathbf{f}_{Di} + \alpha \mathbf{f}_{Li} \quad (2.4)$$

The dual displacement rates at the centroid of the block  $i$ , corresponding by virtual work to the nodal loads  $\mathbf{f}_i$ , are collected in the vector  $\mathbf{u}_i$ :

$$\mathbf{u}_i = \begin{bmatrix} u_{xi} \\ u_{yi} \\ u_{\theta i} \end{bmatrix} \quad (2.5)$$

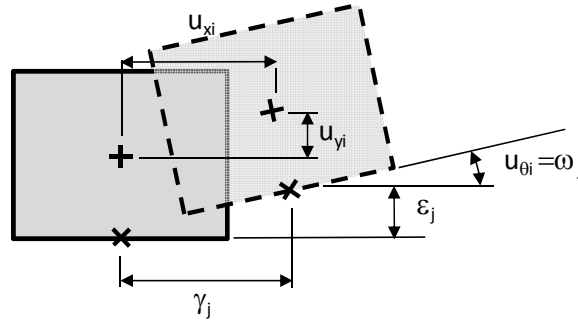


**Figure 2.** Joint and block kinematic variables

## 2.2. Equilibrium equations

For block  $i$  and contact  $j$ , the equilibrium equations can be expressed in the matrix form:

$$\mathbf{A}_{ij} \mathbf{x}_j = \mathbf{f}_i \quad (2.6)$$

where  $\mathbf{A}_{ij}$  is a  $(3 \times 3)$  equilibrium matrix.

For the entire structure the equilibrium in the matrix form gives:

$$\mathbf{A}_{3b \times 3c} \mathbf{x}_{3c} = \mathbf{f}_{3b} \quad (2.7)$$

being  $b$  the number of blocks and  $c$  the number of contacts, and it can be obtained through assembly of matrices for each block.

## 2.3. Constitutive laws for the behaviour of the joints

Different types of failure modes of the joints were considered in this study, namely sliding and crushing failure.

Sliding is governed by a Coulomb type criterion and is expressed by the following relationships:

$$y_j^{s\pm} = \pm \cos \phi V_j - \sin \phi N_j \leq r_{jl} \quad (2.8)$$

where  $y_j^{s\pm}$  are the yield functions for positive and negative sliding,  $\phi$  is the friction angle and  $r_{jl} = c_{jl} \cdot \cos \phi$ , being  $c_{jl}$  the cohesion at joint  $j$ . The friction coefficient is defined as  $\mu = \tan \phi$ .

For separation and crushing, no-tension material with finite material strength and plastic behaviour in

compression was considered. As it is well known, in this case a non-linear yield function is obtained in the space  $M, N$ .

The corresponding parabolic yield condition was approximated by eight hyperplanes. In this case, the generic expression of the admissibility condition for the internal static variables  $M$  and  $N$  at joint  $j$  is:

$$y_j^{ck\pm} = \pm \cos \psi_{jk} M_j - \sin \psi_{jk} N_j \leq r_{jk} \quad \text{for } k=2, \dots, 5 \quad (2.9)$$

In matrix notation, the previous limit conditions at a contact interface  $j$  can be written as:

$$\mathbf{N}_j^T \cdot \mathbf{x}_j \leq \mathbf{r}_j \quad (2.10)$$

being  $\mathbf{N}^T$  the yield function matrix in case of sliding and crushing and  $\mathbf{r}$  a constant vector. The extension of previous expression to the whole structure is straightforward.

## 2.4. Modelling flow rule

The modelling of flow rule has important implications in the formulation of the mathematical program of the limit analysis problem. As mentioned above, this problem results into a linear program in case of associate flow rule and into a mathematical problem with equilibrium constraint in case of non-associate flow rule.

Flow rule provides relationships between plastic multipliers (resultant strain rates) and generalized strains and is governed by the following equations:

$$\mathbf{q} = \mathbf{Vz} \quad (2.11)$$

where  $\mathbf{V}$  is the flow rule matrix and  $\mathbf{z}$  is the vector of plastic multipliers, being  $\mathbf{z} \geq \mathbf{0}$  to ensure energy dissipation of the structural system under applied loads.

In case of associate flow rule ( $\phi = \phi_0$ ), the vector of generalized strains is normal to the yield function  $\mathbf{y}$  ( $\text{grad } \mathbf{y}$ ) and is defined by the following condition:

$$\mathbf{q} = \left( \frac{\partial \mathbf{y}}{\partial \mathbf{x}} \right) \mathbf{z} = (\nabla \mathbf{y}) \mathbf{z} \quad (2.12)$$

For sliding, it can be noted that the generalized plastic strains corresponding to the plastic multiplier  $z_j^{s+}$  are:  $\gamma_j = z_j^{s+} \cos \phi_0$ ;  $\varepsilon_j = -z_j^{s+} \sin \phi_0$ .

Comparing previous equations, it is easy to show that, in case of normality rule, it results:

$$\mathbf{V} = \mathbf{N} \quad (2.13)$$

For non associate flow rule in sliding,  $\mathbf{V}$  can be obtained from previous expressions assuming  $\phi_0 = 0$ .

The definition of the plastic behaviour of joints is completed by the additional condition:

$$\mathbf{y}^T \mathbf{z} = 0 \quad (2.14)$$

known in plasticity as complementarity relation, which allow to have positive components of plastic multipliers  $\mathbf{z}$  only when the stress state is on a yield plane.

## 2.5. Formulation of the limit analysis problem and solution procedure

It is well known that, under the hypothesis of classical plastic theory, which include fully associate plastic flow rules, the lower and upper bound formulations of the limit analysis problem give rise to two dual linear programming problems, static and kinematic, whose unique solution is the load factor  $\alpha$ .

On the basis of previous assumptions, the formulation by linear programming of the static theorem of limit analysis, stating that the collapse load corresponds to the maximum load factor associated to a static admissible distribution of internal forces satisfying yield conditions, is then:

$$\begin{aligned} \max \quad & \alpha \\ \text{subject to: } & \mathbf{A} \cdot \mathbf{x} = \mathbf{f}_D + \alpha \mathbf{f}_L \\ & \mathbf{N}^T \cdot \mathbf{x} \leq \mathbf{r} \end{aligned} \quad (2.15)$$

In case of non-associate flow rule for sliding, the iterative solution procedure proposed by Gilbert et al. (2006) was used to find the minimum collapse load, rather than solving the underlying mixed complementarity program which arise from the limit analysis problem in this case by collecting all previous conditions.

The procedure consists in the solution of a series of linear programming problems with fictitious and variable values of the friction angle and cohesion. Fictitious values of cohesion and angle of friction are used to rotate the yield surface orientation so as to restore the normality to the model and to improve the convergence of the procedure.

In particular, at each iteration, sliding behaviour of joints is governed by a Mohr-Coulomb failure surface with an effective cohesion intercept and variable value of the angle of friction relaxing from small negative values to zero, so to imply a final zero dilatancy. Cohesion values at each iteration are computed on the basis of normal forces calculated in the previous iteration. Starting values of normal forces are obtained from an initial associate friction solution.

## 3. THE RIGID BLOCK MODEL OF THE SHEAR WALL WITH OPENING

On the basis of the developed limit analysis software package, a rigid block model of the brick masonry shear walls tested by Foraboschi (2009) was generated.

The test structures were single-story full-scale unreinforced brick masonry walls with opening, assembled by hydrated lime mortar. Each specimen was composed of two piers, two spandrels and a lintel beam. The frames were composed of double width brick masonry, with nominal dimensions of clay bricks of 250.0 mm in length, 125.0 mm in width, and 61.0 mm in thickness. Five masonry textures were adopted for tests, with different number of transverse bricks.

The experimental tests considered in this paper are those relevant to the specimens with the percentage of bricks set with the larger side across the wall thickness with respect to the wall surface equal to 10.0%, that is the average value among the considered textures.

The walls dimensions and a specimen elevation are shown in Figure 3.

The  $f_{cm}$  compressive strength of masonry measured from standardized tests was 1.21 MPa. The tensile strength was 0.05 MPa and the modulus of elasticity was 1360 MPa.

The specimens were loaded with a constant vertical force and then a horizontal force, applied at the 194 mm height concrete distribution beam poured on the top of each wall, was monotonically increased up to reaching the collapse of the walls.

Three levels of the vertical load  $F_v$  were applied:  $F_v = 40$  kN,  $F_v = 80$  kN and  $F_v = 140$  kN.

The rigid block model of the considered specimens was generated using a simplified micro-modelling approach.

The block dimensions of the numerical model used for the piers and the spandrels are  $260.0 \times 75.6$  mm. The lintel was modelled with rigid blocks of  $226.8 \times 65.0$  mm. The concrete beam at the top of the wall was modelled with a single rigid block.

Masonry material model parameters were deduced from experimental tests and are shown in Table

3.1. For concrete beam, a volumetric weight of 25 kN/m<sup>3</sup> was assumed. The flow rule assumed for sliding is non-associate.

**Table 3.1.** Rigid block model parameters

Compressive strength, $f_m$ [MPa]	Self weight, $\gamma_m$ [kN/m <sup>3</sup> ]	Friction coefficient, $\mu$
1.21	18.0	0.60

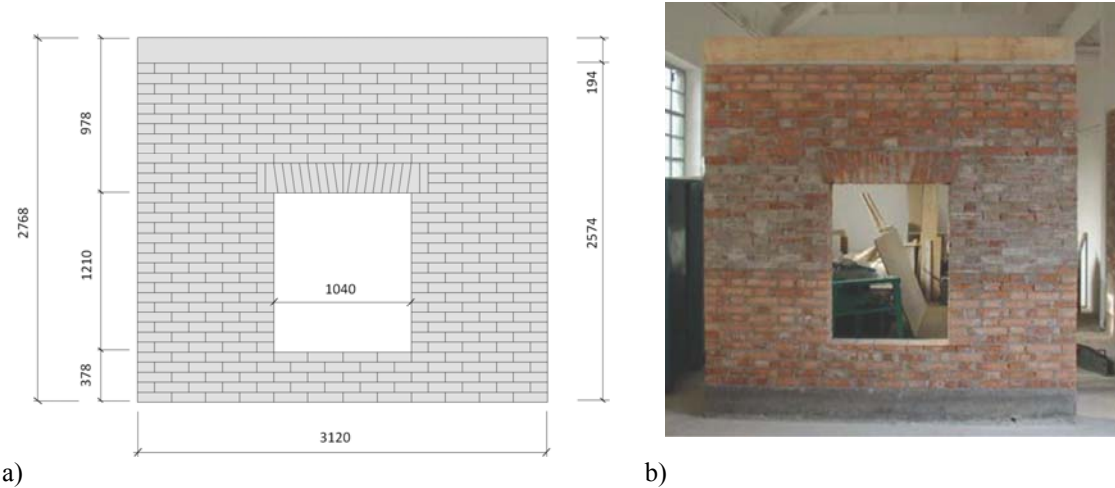


**Figure 3.** a) Model dimensions; b) Specimen elevation (Foraboschi 2009)

The collapse mechanism that have been obtained for the different values of the vertical load are shown in Figures 4 and 5. Two types of mechanisms can be noted.

The first mechanism involves sliding of the spandrel, with the formation of a diagonal crack. The second type is a rocking mechanism and consists in the formation of three rigid macro-blocks rotating about their hinges. In particular, this mechanism involves the rocking of the two piers and the cracking of the spandrel. For  $F_v=140$  kN, extensive crushing is observed at the corners of the right pier as well. The sliding at the lintel observed for  $F_v=80$  kN is prevented for higher values of the vertical force by the larger value of internal friction forces.

A schematization of the collapse mechanism with rigid macro-block for  $F_v=80$  kN and  $F_v=140$  kN is depicted in Figure 6.

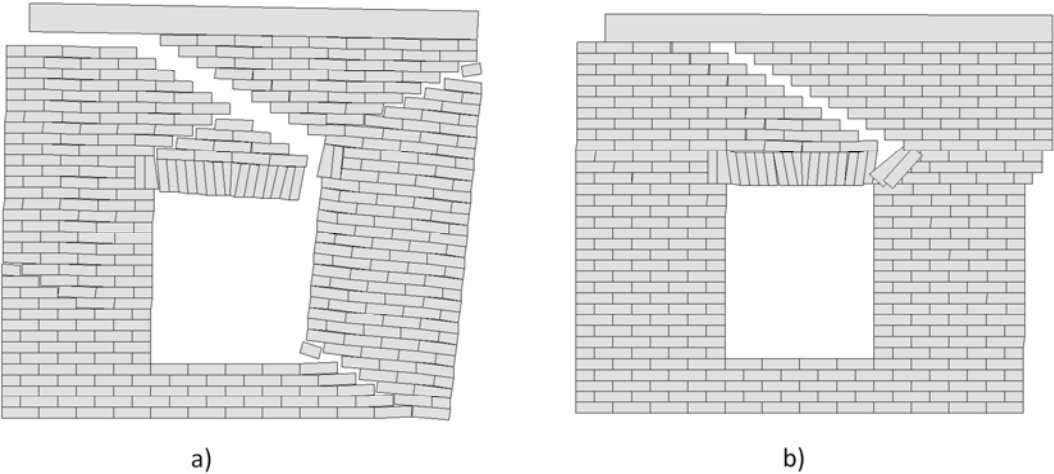


**Figure 4.** Associate and non-associate solutions for  $F_v=40$  kN.  $\mu =0.6$

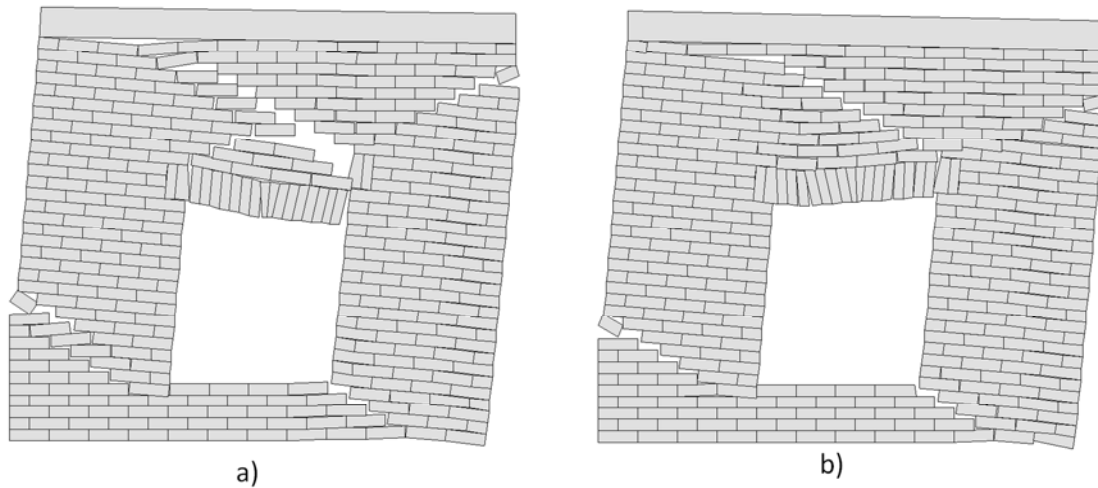


**Figure 5.** Collapse mechanisms for different values of vertical load (non associative friction law,  $\mu=0.6$ ).  
a)  $F_v=80\text{kN}$ ; b)  $F_v=140\text{ kN}$

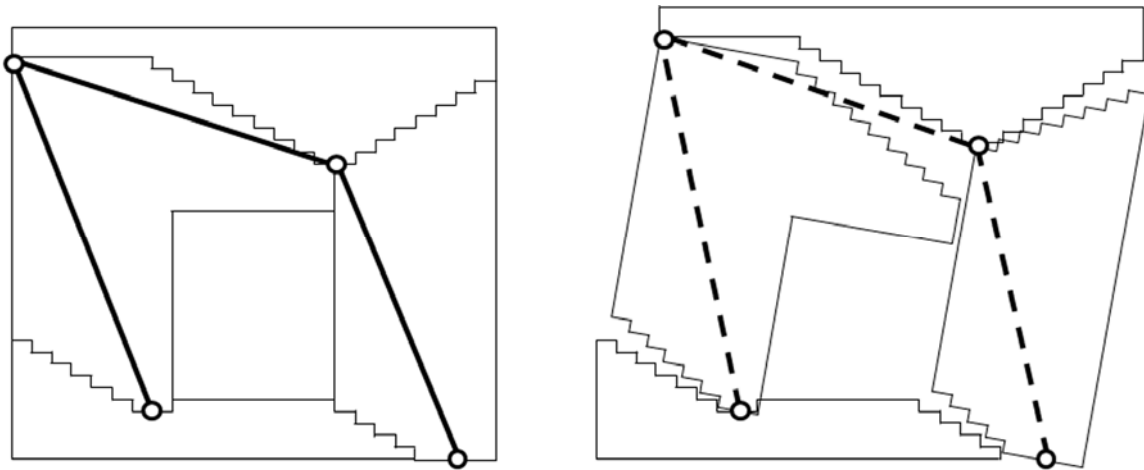


**Figure 6.** Schematisation of the collapse mechanism with rigid macro-blocks

#### 4. COMPARISON OF EXPERIMENTAL AND NUMERICAL RESULTS

To assess the accuracy of the rigid block model, the comparison of experimental and numerical results is shown in this section.

Visual inspections of the specimens after tests revealed that first cracking occurred at the construction joint between the piers and the bottom spandrel. First considerable damage was a diagonal crack that appeared in the leeward top nodal panel. Crack initialized at the center of the nodal panel and propagated diagonally until it reached the upper and lower corners of the nodal panel. Cracks in the spandrel and at the lintel were observed as well (Fig. 7).

It can be noted that the large cracks that developed at the base of the piers and at the spandrel are well predicted by the numerical model.



**Figure 7.** Crack pattern after test 1–3 and 3–5 (Foraboschi 2009)

The comparison of experimental and failure loads predicted with the rigid block model is shown in Table 4.1. A good prediction of the ultimate loads was obtained also in this case.

**Table 4.1.** Test results for the set of three walls with  $P_v=40, 80$  and  $140$  kN and predicted failure load

Wall label	$F_{max}$ [kN]	Rigid block model [kN]
1-3	23.6	23.90
2-3	38.8	39.84
3-3	61.3	55.77

## 5. SENSITIVITY ANALYSIS AND SIMPLIFIED MODELLING STRATEGIES

Sensitivity analysis to model parameters and block arrangements was carried out to assess the stability and robustness of the numerical model.

The material model parameters considered for sensitivity analysis were the angle of friction and the compressive strength. Moreover, different yield functions were considered for compressive and bending behaviour, comparing crushing with rocking for infinite compressive strength. Finally, a simplified micro-model of the specimen was generated with a single block for the lintel.

To analyze the influence of material model parameter on the predicted response, a sensitivity analysis was carried out varying the angle of friction in the range 0.4-0.8. The sensitivity to friction angle was evaluated in terms of collapse load and failure mechanism, considering both associative and non-associative models.

In Figure 8, the variation of the failure load  $F_L$  normalized to the value  $F_{L0}$  corresponding to  $\mu=0.4$  is plotted. The results show that the sensitivity of the model increases as vertical load decreases. In each case, the results show the stability and the robustness of the model.

It is worth the note that, for the specimen loaded under the vertical force of  $F_v=40$ kN, small changes in the angle of friction from the reference value of 0.6 to 0.75 make the collapse mechanism turn from sliding into a rocking mechanism, with slightly differences in the failure load. Being different types of collapse mechanism activated for quite similar values of failure load, this behaviour could be regarded as a sort of ‘instability’ of the collapse mechanism with respect to the failure load, which could be ascribed to the load test itself rather than to the numerical model.

A similar behaviour was noted varying the value of compressive strength in the model.

To compare associative and nonassociative solutions for sliding, in Figure 9 the ratio  $F_{L,ass}/F_L$  as a function of  $\mu$  is shown, being  $F_{L,ass}$  the failure load corresponding to the associative behaviour. Differences observed in the solution of associative and non-associative sliding models are relevant for low value of the vertical load only, when sliding mechanism is predominant.



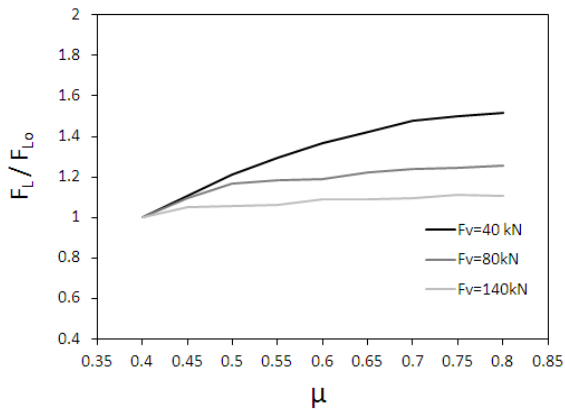


**Figure 8.** Variation of failure load for different values of friction coefficient and  $F_v$

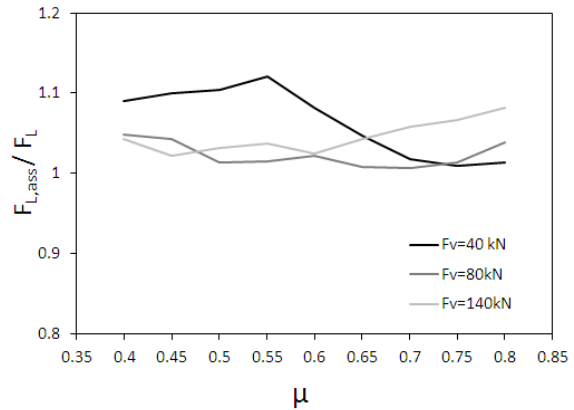


**Figure 9.** Associative and nonassociative solutions

A set of analysis was carried out in order to compare the effect of different modelling assumptions on the compressive and bending interaction at joints, using rocking instead of crushing behaviour. In case of rocking, that is for infinite compressive strength, it was noted that the collapse mechanism predicted by the numerical model does not fit the experimental outcome. Moreover, in this case the differences of associative and nonassociative solutions are remarkable.

Finally, the sensitivity of the model to different simplified micro-modelling approaches was investigated as well. It is well known that the response of this type of model is sensitive to blocks texture. Being focused on micro-modelling, the variation of the predicted response to different block arrangements and size was out the scope of the present paper. Anyway, it was interesting to compare the results when different approach are used for the lintel. The modelling of the lintel is commonly carried out with a single rigid block or with arch structures.

In Figure 10, the comparison of the analysis results obtained on the model of the shear wall with a single rigid block for the lintel is shown.

A different collapse mechanism is observed in this case, although failure load is slightly affected.

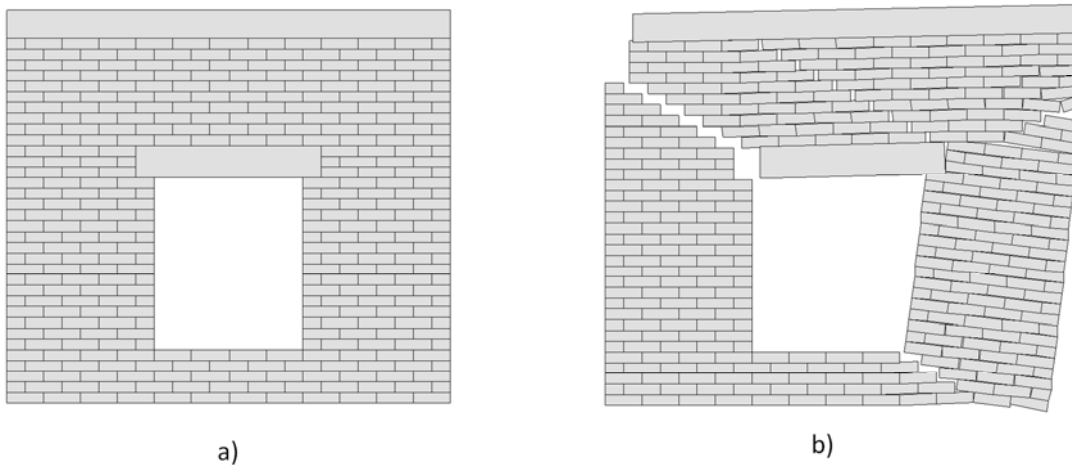


**Figure 10.** a) Rigid block model with a single block for the lintel. b) Predicted failure mechanism

## 6. CONCLUSIONS

In this report an application of rigid block limit analysis to a load test on a perforated masonry shear wall was presented. A micro-modelling approach was used to develop the model of the panels under investigation.

Comparison of experimental and numerical results allowed to evaluate the reliability of the used modelling approach. A good agreement in terms of collapse load and mechanism was observed.

The sensitivity analysis to material model parameters showed that the model is robust and that response is slightly affected by model parameters.

The comparison of associative and nonassociative solutions showed that differences in terms of collapse mechanisms and failure loads increase with decreasing of the level of vertical forces.

The use of a rocking model for the compressive and bending behaviour of joints involves a different collapse mechanism from the crack pattern observed in experimental tests. Moreover, in this case the difference of associative and nonassociate solutions increases remarkably in terms of failure loads.

The failure mechanism predicted by the numerical model is affected by the use of micro or macromodelling for the lintel. More accurate micro-modelling could be used, as variable inclination of blocks.

The mechanism suggests macro-modelling strategies that should be investigated more in detail in further studies.

## REFERENCES

- Ferris, M., Tin-Loi, F. (2001). Limit analysis of frictional block assemblies as a mathematical program with complementarity constraints. *International Journal of Mechanical Sciences* **43**, 209–224.
- Foraboschi P. (2009). Coupling effect between masonry spandrels and piers. *Materials and Structures* **42**:279–300.
- Gilbert, M., Casapulla, C., and Ahmed, H. M. (2006). Limit analysis of masonry block structures with non-associative frictional joints using linear programming. *Computers and Structures*, **84**:873–887.
- Orduña, A., 2003. Seismic assessment of ancient masonry structures by rigid blocks limit analysis. Ph.D. thesis, University of Minho, Guimaraes, Portugal.
- Orduña, A., Lourenço, P.B., 2005. Three-dimensional limit analysis of rigid blocks assemblages. Part I: torsion failure on frictional joints and limit analysis formulation. *Int. J. Solids and Structures* 42 (18-19), 5140-5160.